Supporting Information of

Plasma-chemical promotion of catalysis for CH_4 dry reforming: unveiling plasma-enabled reaction mechanisms

Zunrong Sheng, Hyun-Ha Kim, Shuiliang Yao, Tomohiro Nozaki*

1 Department of Mechanical Engineering, Tokyo Institute of Technology, Tokyo 152-8550, Japan
2 National Institute of Advanced Industrial Science and Technology, Tsukuba 305-8569, Japan
3 School of Environmental and Safety Engineering, Changzhou University, Changzhou 213164, China

*Corresponding author: Tomohiro Nozaki: nozaki.t.ab@m.titech.ac.jp

S1. The effect of Helium on plasma chemistry

Practically, helium must be avoided for economic reason. The role of helium is "diluent gas" (or called "balance gas") in plasma-assisted DRIFTS (diffuse reflectance infrared Fourier transform spectroscopy) experiment. The diluent gas is necessary in IR experiment to dilute the reaction gases. Otherwise, the high concentration of reaction gases will lead an uncontrollable signal saturation of IR spectra [1], which is not favor for in situ measurement. Another technical reason is that helium can decrease the applied voltage significantly which minimizes electromagnetic noise during plasma-DRIFTS experiment. There are some similar plasma-IR studies with diluent gas, e.g., helium [2], and argon [1, 3, 4].

The important gas phase plasma chemistry is the secondary reactions induced by metastable helium. Because the excitation threshold of metastable helium is high (19.84 eV), Penning ionization of CO_2 (or CH_4), stepwise ionization of metastable helium, and the charge transfer of He^+ ions with CO_2 (or CH_4) become significant besides electron impact inelastic collision [5, 6]. Although electron density increases by metastable helium, it does not produce vibrationally excited species.

Yuan *et al* performed numerical simulation of atmospheric pressure homogeneous helium discharge with a trace N_2 [6]. The largest electric field was formed in the plasma sheath, showing 4 kV/cm which corresponds to the reduced electric field of 20 Td at 600 Torr and 300 K [6]. The mean electron energy in the plasma sheath is as high as 3 eV and it would be around 1 eV in the bulk region. In the case of DBD (dielectric barrier discharge), streamer breakdown occurs which would create larger electric field than homogeneous glow-like discharge. Ramakers *et al* studied discharge behavior of helium and argon DBD with a trace CO_2 (5 vol%) [7]. The gas breakdown voltage decreases remarkably due to the contribution of metastable species. Moreover, CO_2 conversion behavior in Ar and He is essentially unchanged, indicating that mean electron energy is smaller than 5 eV. In overall, helium would increase electron number density

via metastable species, but mean electron energy and thus electron collision kinetics would not change to a large extent.

S2. Ex situ CO_2-temperature programmed desorption

Ex situ CO_2-TPD (temperature programmed desorption) was performed in a quartz tube reactor, a temperature controllable furnace and a quadruple mass spectrometer (QMS, Prisma-100; Pfeiffer Vacuum GmbH), which are depicted in Figure S1 [8, 9]. The catalyst pellet of Ni/Al_2O_3 or $La\text{-}Ni/Al_2O_3$ (ca. 11 g) was pretreated by H_2/Ar flow (100/1000 mL/min) at 600 °C for 60 min. CO_2-TPD was carried out based on two control groups at 500 °C with 500 cm^3/min CO_2 flow: plasma CO_2 treatment (*SEI* = 2.7 eV/molecule) and thermal CO_2 treatment. After 60 min of thermal/plasma CO_2 treatment, a rapid cooling program was carried out with a rate of ca. 50 ℃/min in an argon atmosphere to avoid surface species desorption during rapid cooling. After the catalyst temperature reached 25 °C, the CO_2-TPD started with 1000 cm^3/min Ar at a heating rate of 10 °C/min. Figure S2 shows the CO_2-TPD patterns of the Ni/Al_2O_3 catalyst, where peaks I' and III' are assigned to carbonate desorption over the interface between Ni and Al_2O_3.

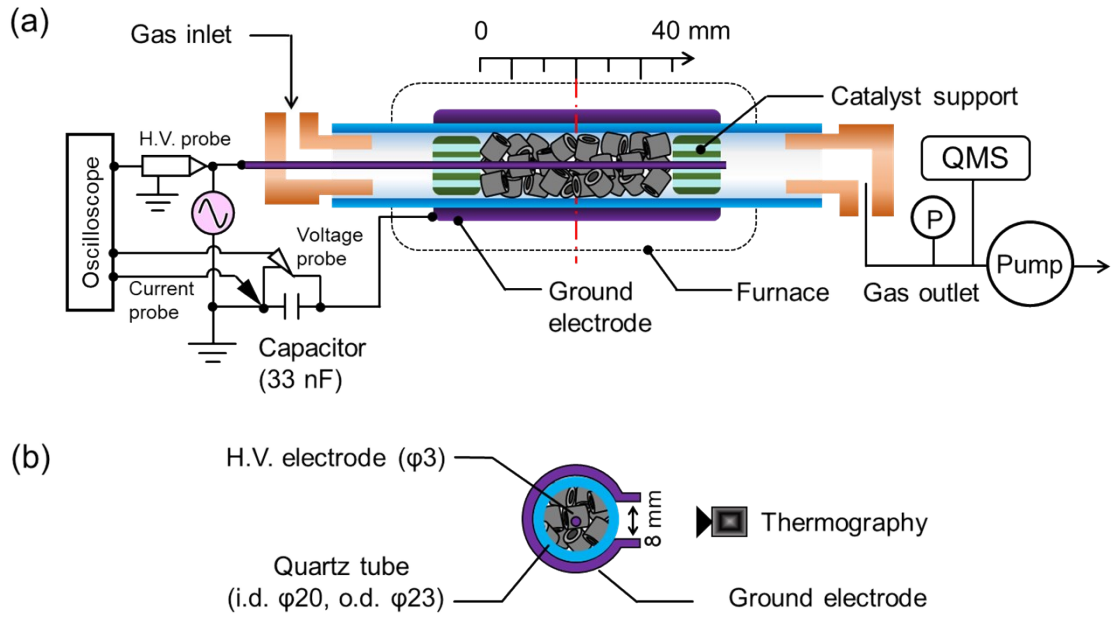

Figure S1. Experimental setup for CO_2-TPD [8, 9].

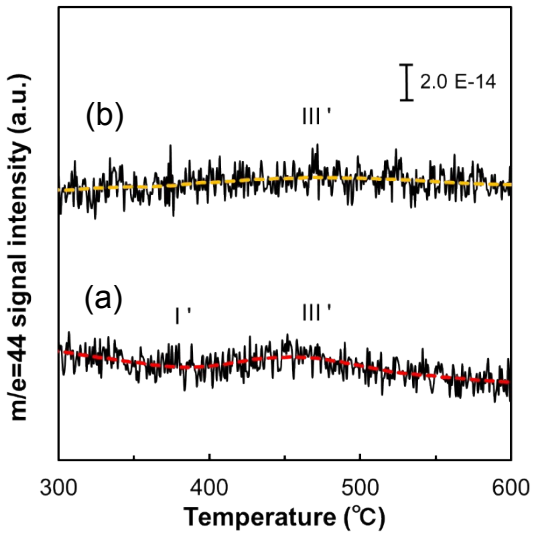

Figure S2. CO_2-TPD patterns of Ni/Al_2O_3 after 500 °C treatment: (a) thermally activated CO_2, (b) plasma-activated CO_2. CO_2 flow rate was 500 mL/min at 10 kPa. Heating rate was 10 °C/min.

S3. Summary of DRIFTS peaks

Table S1 Carbonate structure over the $La-Ni/Al_2O_3$ catalyst and vibration assignments of the DRIFTS peaks

Species	Monodentate carbonate	Bidentate carbonate	Polydentate carbonate	Bridged carbonate	Bicarbonate
Schematic structure*	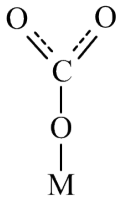	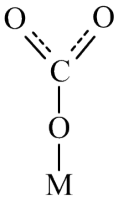	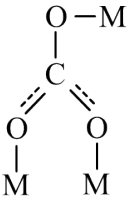	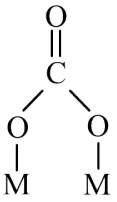	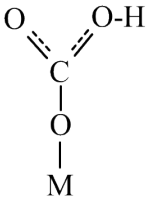
Vibration mode and wavenumber (cm^{-1})	ν_{as} OCO at 1425 cm^{-1}	ν_{as} OCO at 1560 cm^{-1}	ν_{as} CO3 at 1500 cm^{-1}	ν C=O at 1720 cm^{-1}	ν_{as} OCO at 1655 cm^{-1}
	ν_s OCO, at 1345 cm^{-1}	ν_s OCO, at 1290 cm^{-1}			ν OH at 3600-3800 cm^{-1}
Reference	[10-12]	[10]	[13, 14]	[14, 15]	[12, 13, 16-19]

*M represents the coordination metal, lanthanum in this study

S4. CH_4/CO_2 activation over La-Ni/Al_2O_3 at 200 °C

CH_4 was introduced with CO_2 over the carbonate containing La-Ni/Al_2O_3. In spectrum (a) in Figure S3, the gas phase CH_4 was detected as the peaks at 1304 cm^{-1} and 3015 cm^{-1}. The product CO (g), the intermediate species CH_x^* (in the range of 2800 to 3000 cm^{-1} [20, 21]) and CH_xO^* (1750 cm^{-1} [22-24]) were not detected, illustrating that CH_4 dehydrogenation did not occur at 200 °C. In spectrum (b), plasma was employed. The peak at 1560 cm^{-1} (bidentate carbonate) was enhanced slightly by plasma. However, the missing CH_x^* (x=1-3), CH_xO^* and CO (g) imply that plasma at 200 °C is difficult to induce CH_4 chemisorption and dehydrogenation. Besides, the intensity of bidentate carbonate peak at 1560 cm^{-1} was enhanced with plasma-on (spectrum (b)) refers to the scale bar (red color), which corresponds with the results in section 3.1.1.

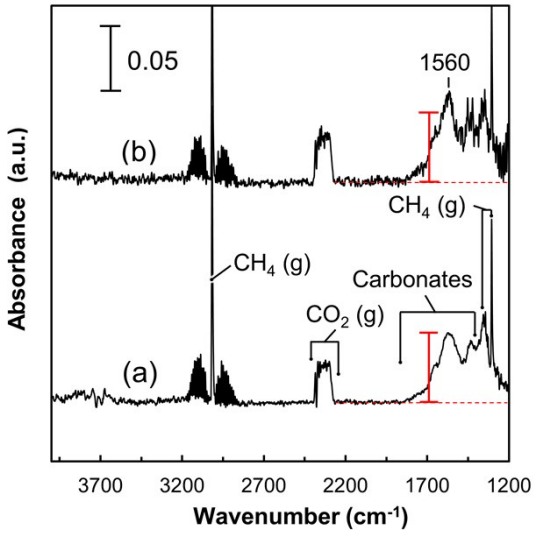

Figure S3. DRIFTS spectra for CO_2/CH_4/He (8.3 vol%, 120 mL/min) activation over La-Ni/Al_2O_3 at 200 °C: (a) plasma-off; (b) plasma-on.

S5. Oxidation-reduction behavior of La-Ni/Al_2O_3

Our previous work confirmed the oxidation-reduction behavior of Ni catalysts by Raman spectroscopy and optical microscopy [13]. The oxidation-reduction behavior enables a change in the transparency of dielectric materials. The absorbance spectra are obtained by the following equation (Beer's law) based on the transmittance spectra in the background measurement.

$$A\,(v) = 2 - \log\,(\%T(v))$$

Here, A and $\%T$ represent the absorbance and percent transmittance, respectively. v represents the wavenumber (cm^{-1}). The absorbance spectra of La-Ni/Al_2O_3 (thermal H_2 reduced sample) and La-NiO/Al_2O_3 (thermal CO_2 oxidized sample) are shown in Figure S4 (a) and (b),

respectively. The spectrum (a) of the reduced sample shows an increase in the profile compared with that of the oxidized sample in the range of 1500~4000 cm^{-1}, as well as 600~800 cm^{-1}, indicating that the absorbance of the infrared signal increases in the case of the H_2-reduced sample (i.e., La-Ni/Al_2O_3). It should be noted that a strong absorbance band is observed in the range of 800~1500 cm^{-1}, which is subtracted as background.

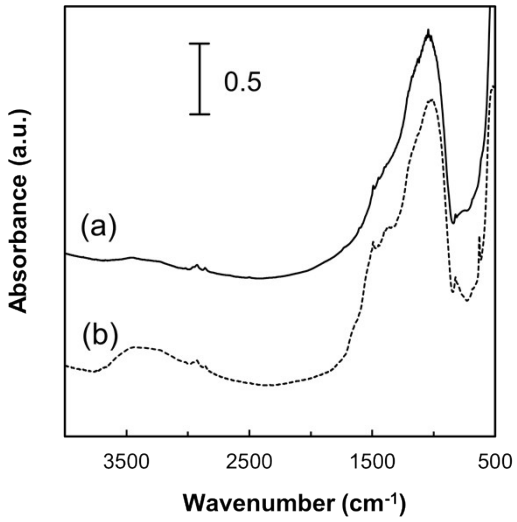

Figure S4. Absorbance spectrum of (a) La-Ni/Al_2O_3 and (b) La-NiO/Al_2O_3 under He flow (100 mL/min) at 600 °C.

In Figure S5, the spectrum recorded at 1 min shows carbonate species (1200-1600 cm^{-1}).-Ni nanocrystals were simultaneously oxidized by thermal CO_2 to NiO. When the H_2 flowed to the DRIFTS cell from 5 min to 15 min instead of CO_2, the baseline lifted upwards, which was attributed to NiO reduction by H_2. Carbonates (between 1200 and 1600 cm^{-1}) were consumed at 5 min and gradually disappeared after 10 min. A weak OH^* band (3700 cm^{-1}) was detected at 5 min in the inset figure. This indicates that OH^* species are the intermediate product when surface hydrogen reacts with carbonates [25] because the decomposition of H_2 easily forms adsorbed H species on Ni [26-28]. The bands of gas phase H_2O (1250 to 2000 cm^{-1} and 3500 to 4000 cm^{-1}) were not clearly detectable, suggesting that H_2O may not be produced via the reduction of NiO or carbonates. After 15 min, CO_2 was introduced instead of H_2, and then the baseline “turned back" to oxidized conditions at 30 min with carbonate peaks, which was similar to the spectrum at 1 min.

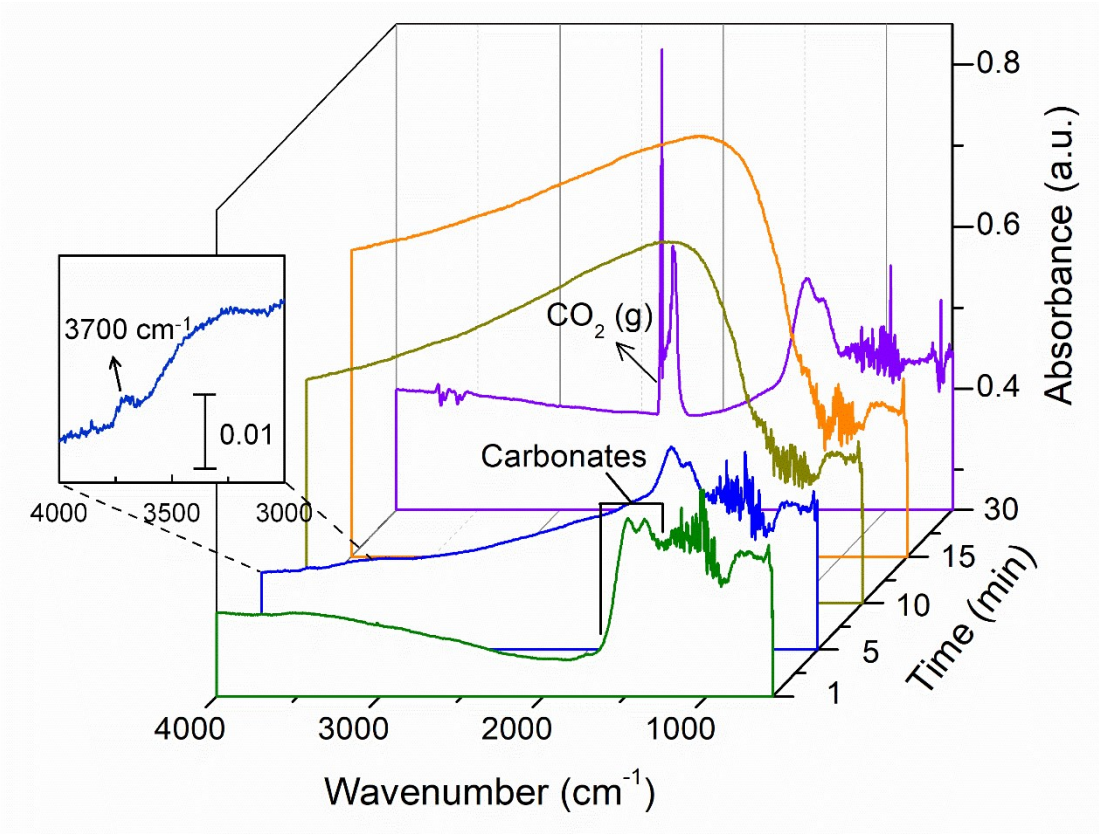

Figure S5. DRIFT spectra of oxidation-reduction behavior on La-Ni/Al_2O_3 at 600 °C: 1 min: oxidized catalyst with CO_2/He (9 vol.%, 110 mL/min) treatment; 5-15 min: reduced catalyst with H_2/He (9 vol.%, 110 mL/min) treatment; 30 min: reoxidized catalyst with CO_2/He (9 vol.%, 110 mL/min) treatment.

References

[1] S. Xu, S. Chansai, Y. Shao, S. Xu, Y.-c. Wang, S. Haigh, Y. Mu, Y. Jiao, C.E. Stere, H. Chen, X. Fan, C. Hardacre, Mechanistic study of non-thermal plasma assisted CO_2 hydrogenation over Ru supported on MgAl layered double hydroxide, Applied Catalysis B: Environmental 268 (2020) 118752.

[2] C.E. Stere, W. Adress, R. Burch, S. Chansai, A. Goguet, W.G. Graham, C. Hardacre, Probing a Non-Thermal Plasma Activated Heterogeneously Catalyzed Reaction Using in Situ DRIFTS-MS, ACS Catalysis 5 (2015) 956-964.

[3] A.J. Knoll, S. Zhang, M. Lai, P. Luan, G.S. Oehrlein, Infrared studies of gas phase and surface processes of the enhancement of catalytic methane decomposition by low temperature plasma, Journal of Physics D: Applied Physics 52 (2019) 225201.

[4] S. Zhang, Y. Li, A. Knoll, G.S. Oehrlein, Mechanistic aspects of plasma-enhanced catalytic methane decomposition by time-resolved operando diffuse reflectance infrared Fourier transform spectroscopy, Journal of Physics D: Applied Physics 53 (2020) 215201.

[5] W. Ning, D. Dai, Y. Zhang, Y. Han, L. Li, Effects of trace of nitrogen on the helium atmospheric pressure

plasma jet interacting with a dielectric substrate, Journal of Physics D: Applied Physics 51 (2018) 125204.

[6] Y. Xiaohui, L.L. Raja, Computational study of capacitively coupled high-pressure glow discharges in helium, IEEE Transactions on Plasma Science 31 (2003) 495-503.

[7] M. Ramakers, I. Michielsen, R. Aerts, V. Meynen, A. Bogaerts, Effect of Argon or Helium on the CO2 Conversion in a Dielectric Barrier Discharge, Plasma Processes and Polymers 12 (2015) 755-763.

[8] Z. Sheng, S. Kameshima, S. Yao, T. Nozaki, Oxidation behavior of Ni/Al2O3 catalyst in nonthermal plasma-enabled catalysis, Journal of Physics D: Applied Physics 51 (2018) 445205.

[9] Z. Sheng, K. Sakata, Y. Watanabe, S. Kameshima, H.-H. Kim, S. Yao, T. Nozaki, Factors determining synergism in plasma catalysis of biogas at reduced pressure, Journal of Physics D: Applied Physics 52 (2019) 414002.

[10] K. Li, X. Chang, C. Pei, X. Li, S. Chen, X. Zhang, S. Assabumrungrat, Z.-J. Zhao, L. Zeng, J. Gong, Ordered mesoporous Ni/La2O3 catalysts with interfacial synergism towards CO2 activation in dry reforming of methane, Applied Catalysis B: Environmental 259 (2019) 118092.

[11] Y. Yan, Y. Dai, H. He, Y. Yu, Y. Yang, A novel W-doped Ni-Mg mixed oxide catalyst for CO2 methanation, Applied Catalysis B: Environmental 196 (2016) 108-116.

[12] X. Jiao, L. Li, N. Zhao, F. Xiao, W. Wei, Synthesis and Low-Temperature CO2 Capture Properties of a Novel Mg–Zr Solid Sorbent, Energy & Fuels 27 (2013) 5407-5415.

[13] S.C. Shen, X. Chen, S. Kawi, CO2 Adsorption over Si-MCM-41 Materials Having Basic Sites Created by Postmodification with La2O3, Langmuir 20 (2004) 9130-9137.

[14] O.V. Manoilova, S.G. Podkolzin, B. Tope, J. Lercher, E.E. Stangland, J.-M. Goupil, B.M. Weckhuysen, Surface Acidity and Basicity of La2O3, LaOCl, and LaCl3 Characterized by IR Spectroscopy, TPD, and DFT Calculations, The Journal of Physical Chemistry B 108 (2004) 15770-15781.

[15] D.A. Constantinou, A.M. Efstathiou, The steam reforming of phenol over natural calcite materials, Catalysis Today 143 (2009) 17-24.

[16] H. Lu, X. Yao, J. Li, S. Yao, Z. Wu, H. Zhang, H. Lin, T. Nozaki, Mechanism on the plasma-catalytic oxidation of graphitic carbon over Au/γ-Al2O3 by in situ plasma DRIFTS-mass spectrometer, Journal of Hazardous Materials 396 (2020) 122730.

[17] X.E. Verykios, Catalytic dry reforming of natural gas for the production of chemicals and hydrogen, International Journal of Hydrogen Energy 28 (2003) 1045-1063.

[18] D. Cornu, H. Guesmi, J.-M. Krafft, H. Lauron-Pernot, Lewis Acido-Basic Interactions between CO2 and MgO Surface: DFT and DRIFT Approaches, The Journal of Physical Chemistry C 116 (2012) 6645-6654.

[19] X. Wang, U.S. Ozkan, Correlation of NO and CO2 adsorption sites with aldehyde hydrogenation performance of sulfided NiMo/Al2O3 catalysts, Journal of Catalysis 227 (2004) 492-501.

[20] J. Guo, H. Lou, L. Mo, X. Zheng, The reactivity of surface active carbonaceous species with CO2 and its role on hydrocarbon conversion reactions, Journal of Molecular Catalysis A: Chemical 316 (2010) 1-7.

[21] J. Zheng, C. Wang, W. Chu, Y. Zhou, K. Köhler, CO2 Methanation over Supported Ru/Al2O3 Catalysts: Mechanistic Studies by In situ Infrared Spectroscopy, ChemistrySelect 1 (2016) 3197-3203.

[22] V. Lochař, FT-IR study of methanol, formaldehyde and methyl formate adsorption on the surface of Mo/Sn

oxide catalyst, Applied Catalysis A: General 309 (2006) 33-36.

[23] Q. Yang, X. Yin, C. Wu, S. Wu, D. Guo, Thermogravimetric-Fourier transform infrared spectrometric analysis of CO2 gasification of reed (Phragmites australis) kraft black liquor, Bioresource Technology 107 (2012) 512-516.

[24] C.-J. Liu, B. Xue, B. Eliasson, F. He, Y. Li, G.-H. Xu, Methane Conversion to Higher Hydrocarbons in the Presence of Carbon Dioxide Using Dielectric-Barrier Discharge Plasmas, Plasma Chemistry and Plasma Processing 21 (2001) 301-310.

[25] A.H. Khoja, M. Tahir, N.A. Saidina Amin, Evaluating the Performance of a Ni Catalyst Supported on La2O3-MgAl2O4 for Dry Reforming of Methane in a Packed Bed Dielectric Barrier Discharge Plasma Reactor, Energy & Fuels 33 (2019) 11630-11647.

[26] J.K. No/rskov, Effective medium potentials for molecule–surface interactions: H2 on Cu and Ni surfaces, The Journal of Chemical Physics 90 (1989) 7461-7471.

[27] C. Zhi, Q. Wang, B. Wang, D. Li, R. Zhang, Insight into the mechanism of methane synthesis from syngas on a Ni(111) surface: a theoretical study, RSC Advances 5 (2015) 66742-66756.

[28] S. Jiang, Y. Lu, S. Wang, Y. Zhao, X. Ma, Insight into the reaction mechanism of CO2 activation for CH4 reforming over NiO-MgO: A combination of DRIFTS and DFT study, Applied Surface Science 416 (2017) 59-68.